A Symmetrical Condensed Node for the TLM Method

PETER B. JOHNS

Abstract —A new symmetrical condensed node is developed for the analysis of electromagnetic waves by the transmission-line modeling (TLM) method of numerical analysis. The new node has the advantage of condensing the field components to one point in space at the node and removes the disadvantage of asymmetry in existing condensed nodes.

I. Introduction

TRANSMISSION-LINE MODELING (TLM) provides a conceptual model which produces a time-domain numerical technique for solving networks and fields [1]. Electromagnetic fields are modeled by filling the field space with a network of transmission lines which renders the problem discrete in space and time since pulses launched on the network scatter from point to point in space in a fixed timestep. The theory and application of TLM for electromagnetic simulation are reviewed in an excellent paper by Hoefer [2], who also describes some of the later developments.

The network of transmission lines shown in Fig. 1 for modeling three-dimensional electromagnetic waves has been developed by interconnecting two-dimensional shunt and series nodes [3]. There is half a timestep delay between these nodes, and for this reason the network is termed an expanded-node network.

The expanded-node network has been used for a variety of applications over many years [2]; it is similar to finite-difference methods in the same way that the TLM method in its application to diffusion is similar to finite differences [4]. A numerical advantage of TLM over the method of Yee [5], for example, is that three of the six field components are available at each node (rather than one), thus making boundary description finer and giving more information at each node. Also, TLM is a one-step method, whereas the finite-difference routine is a two-step method. Conceptually, TLM has the advantage that it is a physical model with an exact computer solution.

The outstanding disadvantage of the expanded-node network and the finite-difference method is that the topology of the network graph is quite complicated. The nodes, where different field components are conveniently calculated, are spatially separated. In the finite-difference method, for example, all six field components are separated [6]. This has made data preparation for the modeling of boundaries difficult and liable to error, and the problem is particularly acute when automatic data preparation schemes are implemented. The process of diakoptics for forming substructures [7], [8] is also difficult to organize because of the half-timesteps and the spatial separation of different polarizations [9].

This inconvenience of the expanded node network has led to the development of a condensed-node structure by Saguet and Pic [10]; this and other improvements in TLM are described in an interesting paper by Saguet and Tedjini [11]. The condensed node has also been evaluated and used independently by Amer [12]. The node is shown in Fig. 2, and it can be seen that the network topology is simply a three-dimensional Cartesian mesh with two lines, corresponding to two polarizations, in each branch. All of the scattering processes take place at one point in space for the node, all of the field components are also at one point in space, and boundary conditions can be applied at the node or halfway between nodes. However, it can also be seen from Fig. 2 that the node is asymmetrical because, depending upon the direction of view, the first connection in the node is either shunt or series. This asymmetry has been carefully investigated by Amer [12], and it has been found that in most problems the errors are insignificant. Nevertheless, it does mean that boundaries viewed in one direction have slightly different properties when viewed in another, especially at high frequencies. The scattering process for this node is obtained in the computer by first calculating the six nodal quantities from the 12 incident pulses and then calculating the 12 reflected pulses. Although this procedure makes the scattering computation efficient, it does involve quite lengthy arithmetic. Nevertheless, in spite of these disadvantages, it has been demonstrated [10]–[12] that the asymmetrical condensed-node technique uses less computer resources than the expanded-node technique.

This paper takes yet another step and describes the development of a symmetrical condensed node for transmission-line modeling of electromagnetic waves. This node eliminates the disadvantages of asymmetry and cumbersome arithmetic in the asymmetrical node while preserving the advantages of condensed-node working.

In this paper, a condensed node without stubs is first considered. The absence of stubs means that extra inductance and capacitance cannot be added locally to the node and so the node represents only a cubic block of homogeneous space in a Cartesian mesh. The paper then gives the

Manuscript received March 20, 1986; revised November 24, 1986.
The author is with the Department of Electrical Engineering, University of Nottingham, University Park, Nottingham NG7 2RD England.
IEEE Log Number 8613284.

0018-9480/87/0400-0370$01.00

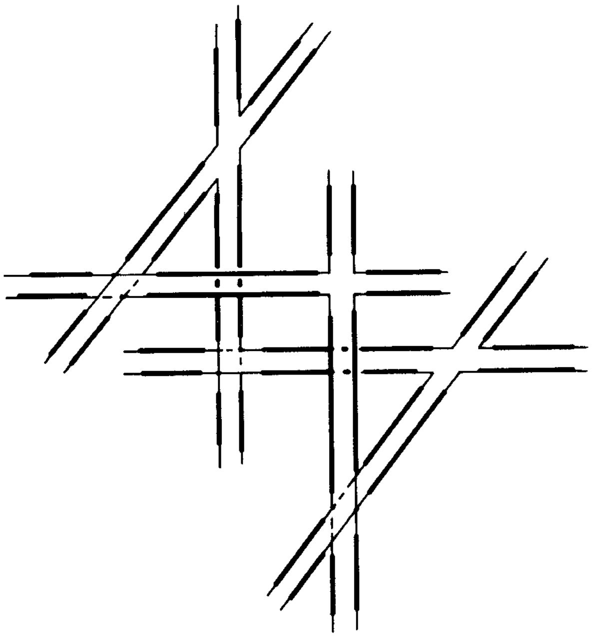

Fig. 1. The expanded node.

scattering matrix for the node with stubs. This allows the node to be used in inhomogeneous problems and in problems described by a completely general orthogonal mesh. The output and excitation properties of the node with stubs are considered and a simple propagation analysis is given for waves propagating in two different directions.

II. The Symmetrical Condensed Node Without Stubs

Hitherto, the method for obtaining the scattering matrix for a node in a transmission-line graph has been to represent the node by an equivalent electrical circuit obtained by replacing transmission-line and incident pulses by Thevenin equivalent circuits. In developing the symmetrical condensed node, it is necessary to make a break with this tradition since the node can no longer be represented by a lumped circuit.

The proposed node without stubs is depicted in Fig. 3. It is convenient to preserve the idea of two-wire transmission lines, and these are shown for convenience on the sides of what can be imagined as square ducts made of insulating material. The two polarizations in any direction of propagation are carried on two pairs of transmission lines which do not couple with each other. In the expanded mesh, these two transmission lines are totally separated in space.

The 12 transmission lines all have the same characteristic impedance, which also equals the characteristic impedance of free space, Z_0. These lines link the Cartesian mesh of nodes together and are termed link transmission lines. Twelve pulses on the link transmission lines, incident upon the node, produce scattering into 12 reflected pulses. The incident and reflected pulses appear on the terminals of the transmission lines at ports which are numbered and directed according to the voltages shown in Fig. 3.

Let the scattering be defined by

$$V^r = SV^i$$

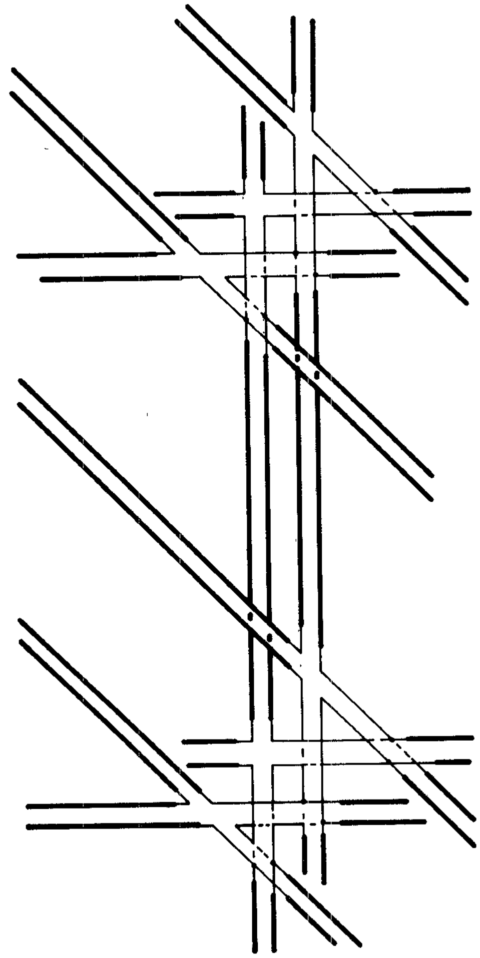

Fig. 2. The asymmetrical condensed node.

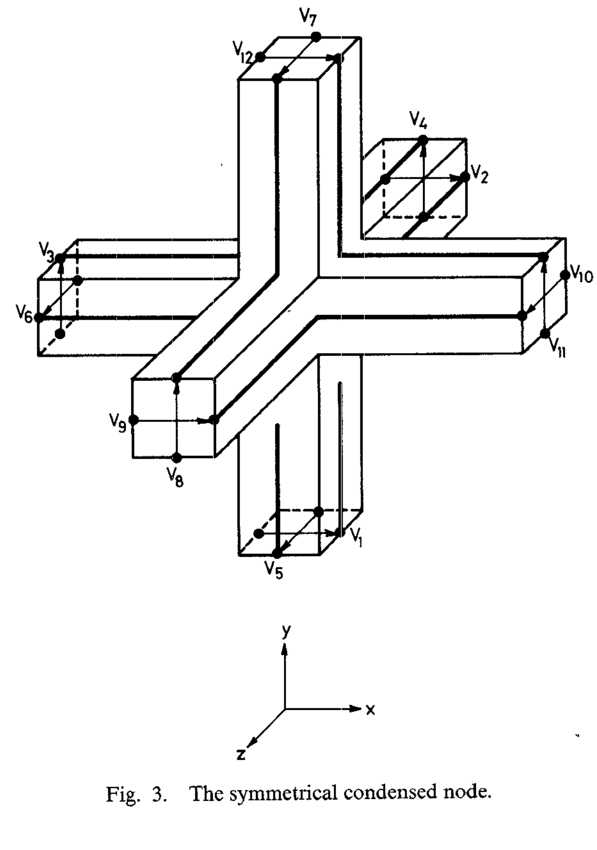

Fig. 3. The symmetrical condensed node.

where $\boldsymbol{S}$ is a 12×12 matrix with elements S_{mn} in the mth row and nth column.

Suppose that a voltage pulse V_1^i of unit amplitude is incident upon port 1 of the structure in Fig. 3. The pulse proceeding toward the junction has associated with it the field quantities E_x and H_z. One of Maxwell's equations involving coupling between these two fields is

$$\frac{\partial H_z}{\partial y}-\frac{\partial H_y}{\partial z}=\epsilon\frac{\partial E_x}{\partial t}. \tag{1}$$

This equation requires that the pulse incident on port 1 scatter into ports 1, 2, 9, and 12 since E_x and H_z are also associated with port 12 on a y-directed line, and E_x and H_y are associated with ports 2 and 9 on z-directed lines. Let the amplitudes of the pulses scattered into ports 1 and 12 be a and c, respectively. If a symmetrical node exists, then the pulses scattered into ports 2 and 9 must be equal, and the variable b is assigned to these.

The other equation of Maxwell's involving E_x and H_z is

$$\frac{\partial E_y}{\partial x}-\frac{\partial E_x}{\partial y}=-\mu\frac{\partial H_z}{\partial t}. \tag{2}$$

This means that pulses are also scattered into ports 3 and 11, and if the symmetrical node exists, these will be equal and opposite in sign. The variable d is assigned to the pulse scattered into port 3 and $-d$ to the one into port 11.

If the same procedure is applied to all ports, then the scattering matrix $\boldsymbol{S}$ may be written as

$$\boldsymbol{S}=\begin{bmatrix}
a & b & d & 0 & 0 & 0 & 0 & 0 & b & 0 & -d & c\\
b & a & 0 & 0 & 0 & d & 0 & 0 & c & -d & 0 & b\\
d & 0 & a & b & 0 & 0 & 0 & b & 0 & 0 & c & -d\\
0 & 0 & b & a & d & 0 & -d & c & 0 & 0 & b & 0\\
0 & 0 & 0 & d & a & b & c & -d & 0 & b & 0 & 0\\
0 & d & 0 & 0 & b & a & b & 0 & -d & c & 0 & 0\\
0 & 0 & 0 & -d & c & b & a & d & 0 & b & 0 & 0\\
0 & 0 & b & c & -d & 0 & d & a & 0 & 0 & b & 0\\
b & c & 0 & 0 & 0 & -d & 0 & 0 & a & d & 0 & b\\
0 & -d & 0 & 0 & b & c & b & 0 & d & a & 0 & 0\\
-d & 0 & c & b & 0 & 0 & 0 & b & 0 & 0 & a & d\\
c & b & -d & 0 & 0 & 0 & 0 & 0 & b & 0 & d & a
\end{bmatrix}$$

and the problem now is to determine the values of a, b, c, and d.

Let the node represent a block of space of dimensions u, v, and w, as shown in Fig. 4 and let the total capacitance associated with transmission lines 1, 2, 9, and 12 be C_x, where

$$C_x=\epsilon\frac{wv}{u}. \tag{3}$$

Let the fields associated with these lines be

$$E_x=V_x/u$$
$$H_y=I_z/v$$
$$H_z=-I_y/w \tag{4}$$

where V_x is the voltage drop across the transmission lines in the x direction. I_y and I_z are currents circulating in transmission lines in the y and z directions, respectively, and are mesh currents or common currents [13].

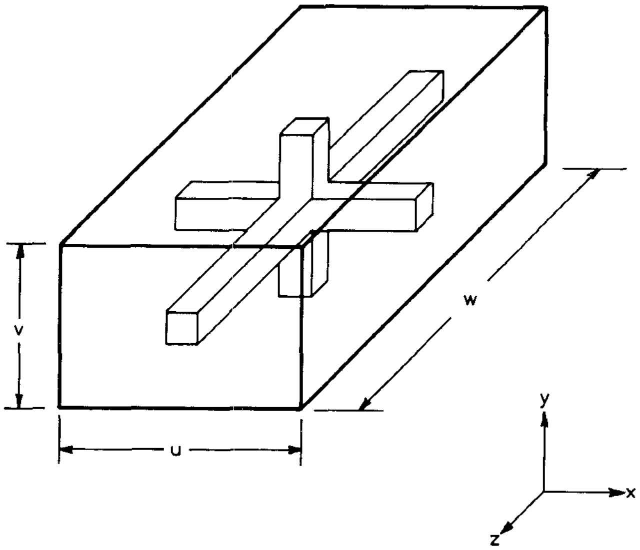

Fig. 4. Representation of space by the condensed node.

Let I_1, I_2, I_9, and I_{12} be the currents entering ports 1, 2, 9, and 12, respectively. Then the discrete form of (1) becomes

$$\frac{I_{12}+I_1}{wv}+\frac{I_9+I_2}{wv}=\frac{C_xu}{wv}\frac{\partial}{\partial t}\frac{V_x}{u}$$

i.e.,

$$I_{12}+I_1+I_9+I_2=C_x\frac{\partial V_x}{\partial t}. \tag{5}$$

Equation (5) indicates that the only loss of current entering the four ports must be due to the rate of change of voltage across the capacitance of the transmission lines and there must be no loss of current at the node.

The scattering matrix could be expressed in terms of voltages, currents, field quantities, or a combination of these. Historically, the voltage has been used, and it is convenient to continue with this convention. Thus, in terms of voltage pulses on link lines of equal characteristic impedance, the conservation of current at the node requires that

$$1 - a = 2b + c. \tag{6}$$

Referring again to Figs. 3 and 4, the inductance associated with transmission lines 1, 3, 11, and 12 is L_z, where

$$L_z = \mu \frac{uv}{w} \tag{7}$$

and the associated fields are

$$E_x = V_x/u$$
$$E_y = V_y/v$$

and

$$H_z = I_z/w.$$

$$S = \frac{1}{2}\begin{bmatrix}
 & 1 & 1 & & & & & & 1 & & -1 & \\
1 & & & & & 1 & & & & -1 & & 1 \\
1 & & & 1 & & & & 1 & & & & -1 \\
 & & 1 & & 1 & & -1 & & & & 1 & \\
 & & & 1 & & 1 & & -1 & & 1 & & \\
 & 1 & & & 1 & & 1 & & -1 & & & \\
 & & & -1 & & 1 & & 1 & & 1 & & \\
 & & 1 & & -1 & & 1 & & & & 1 & \\
1 & & & & & -1 & & & & 1 & & 1 \\
 & -1 & & & 1 & & 1 & & 1 & & & \\
-1 & & & 1 & & & & 1 & & & & 1 \\
 & 1 & -1 & & & & & & 1 & & 1 &
\end{bmatrix} \tag{14}$$

Here, I_z is the mesh current or common current associated with the four transmission lines. Note that the method of solution of the transmission-line structure uses pulses, this forces the currents on each of the two individual wires of each transmission line to be equal and opposite, which automatically sets to zero the type-W mesh currents discussed in [13].

Let V_1, V_3, V_{11}, and V_{12} be the voltages across ports 1, 3, 11, and 12, respectively. Then the discrete form of (2) is

$$\frac{V_{11} - V_3}{uv} - \frac{(V_{12} - V_1)}{uv} = -L_z \frac{w}{uv} \frac{\partial}{\partial t} \frac{I_A}{w}$$

i.e.,

$$V_3 + V_{12} - V_{11} - V_1 = L_z \frac{\partial I_A}{\partial t}. \tag{8}$$

Equation (8) indicates that the only loss of voltage across the four ports must be due to the rate of change of current in the inductance of the transmission lines and there must be no loss of voltage at the node. Thus,

$$1 + a = 2d + c. \tag{9}$$

For loss-free propagation of waves, the node must conserve energy under all combinations of incident pulse excitation, and this leads to the requirement that the scattering matrix be a unitary matrix [14], i.e.,

$$S^T S = I.$$

Thus,

$$\sum S_{nr} S_{ns} = 1 \qquad r = s$$

and

$$\sum S_{nr} S_{ns} = 0 \qquad r \neq s$$

which gives the following equations:

$$a^2 + 2b^2 + c^2 + 2d^2 = 1 \tag{10}$$
$$2ab + 2bc = 0 \tag{11}$$
$$2ad - 2cd = 0 \tag{12}$$
$$2ac + 2b^2 - 2d^2 = 0. \tag{13}$$

It is interesting to find that (10)–(13) do have a solution and this solution also satisfies (6)–(9). It is

$$a = 0 \quad c = 0 \quad b = \tfrac{1}{2} \quad d = \tfrac{1}{2}.$$

The scattering matrix becomes (14), which is a remarkably simple and satisfying result.

III. The Symmetrical Condensed Node with Stubs

The node with stubs has six extra ports. Ports 1–12 are exactly the same as for the node without stubs and are connected to neighboring nodes to form the mesh. The stub ports 13, 14, 15, 16, 17, and 18 couple only with the fields E_x, E_y, E_z, H_x, H_y, and H_z, respectively. The E-field stub ports are open circuit and add capacitance to the node, while the H-field stub ports are short circuit and add inductance to the node. The time taken for a pulse to travel from the port terminals to the center of the node where scattering takes place is $\Delta t/2$ for all transmission-line legs 1–18, where Δt is the TLM timestep.

Let Y_x be the characteristic admittance of the E_x stub normalized to the characteristic admittance of free space (Y_0). Let L_d and C_d be the distributed inductance and capacitance (i.e., the inductance and capacitance of the stub per unit length) and let the length of the stub be $\Delta l/2$. The capacitance of the E_x stub is then given by

$$C_{sx} = C_d \frac{\Delta l}{2} = C_d \frac{\Delta t}{2\sqrt{\mu_0 \epsilon_0}}.$$

Also,

$$\sqrt{\frac{C_d}{L_d}} = Y_x \sqrt{\frac{\epsilon_0}{\mu_0}} \text{ and } \frac{1}{\sqrt{L_d C_d}} = \frac{1}{\sqrt{\mu_0 \epsilon_0}}$$

$$C_d = Y_x \epsilon_0$$

i.e.,

$$C_{sx} = Y_0 Y_x \frac{\Delta t}{2}. \tag{15}$$

A similar analysis can be made for all of the transmission-line legs and the results are summarized in Table I.

The scattering matrix is found by extension of the principles of the previous section. Since, by definition, the voltage pulse incident on port 13 only couples with the E_x field, it will scatter into ports 1, 2, 9, and 12. This amplitude is taken to be e, and the amplitude scattered back into itself is taken to be h. Also, pulses incident on ports 1, 2, 9, and 12 will couple into port 13, and this amplitude is taken to be g. All these variables will be associated with Y_x, the characteristic admittance of the E_x stub on port 13. Pulses incident on ports 3, 4, 8, 11, and 14 will have similar variables associated with Y_y, and pulses incident on ports 5, 6, 7, 10, and 15 are associated with Y_z. Similar arguments apply to the inductance stubs on ports 16, 17, and 18.

The scattering equation

$$V^r = S V^i \tag{16}$$

for the node with stubs now contains an 18×18 scattering matrix which takes the following form. The association of the rows and columns with the particular Y and Z parameters is indicated.

TABLE I
LINK AND STUB TRANSMISSION-LINE INDUCTANCE AND CAPACITANCE

Leg No.	Type	Inductance	Capacitance
1–12	Links	$Z_0 \Delta t/2$	$Y_0 \Delta t/2$
13	E_x Stub		$Y_0 Y_x \Delta t/2$
14	E_y Stub		$Y_0 Y_y \Delta t/2$
15	E_z Stub		$Y_0 Y_z \Delta t/2$
16	H_x Stub	$Z_0 Z_x \Delta t/2$	
17	H_y Stub	$Z_0 Z_y \Delta t/2$	
18	H_z Stub	$Z_0 Z_z \Delta t/2$	

Current and voltage conservation, together with the unitary conditions, has been applied as before. After some manipulation, the values of the parameters in the scattering matrix are found to be

$$a = \frac{-Y}{2(4+Y)} + \frac{Z}{2(4+Z)}$$
$$b = \frac{4}{2(4+Y)}$$
$$c = \frac{-Y}{2(4+Y)} - \frac{Z}{2(4+Z)}$$
$$d = \frac{4}{2(4+Z)}$$
$$e = b$$

Row No.	Associated s/c Stub (Y)	Associated o/c Stub (Z)	1	2	3	4	5	6	7	8	9	10	11	12	13	14	15	16	17	18
Column No.			1	2	3	4	5	6	7	8	9	10	11	12	13	14	15	16	17	18
Associated s/c Stub (Y)			x	x	y	y	z	z	z	y	x	z	y	x	x	y	z			
Associated o/c Stub (Z)			z	y	z	x	x	y	x	x	y	y	z	z				x	y	z
1	x	z	a	b	d						b		$-d$	c	g					i
2	x	y	b	a				d			c	$-d$		b	g				$-i$	
3	y	z	d		a	b				b			c	$-d$		g				$-i$
4	y	x			b	a	d		$-d$	c			b			g		i		
5	z	x				d	a	b	c	$-d$		b					g	$-i$		
6	z	y		d			b	a	b		$-d$	c					g		i	
7	z	x				$-d$	c	b	a	d		b					g	i		
8	y	x			b	c	$-d$		d	a			b			g		$-i$		
9	x	y	b	c				$-d$			a	d		b	g				i	
10	z	y		$-d$			b	c	b		d	a					g		$-i$	
11	y	z	$-d$		c	b				b			a	d		g				i
12	x	z	c	b	$-d$						b		d	a	g					$-i$
13	x		e	e							e			e	h					
14	y				e	e				e			e			h				
15	z						e	e	e			e					h			
16		x				f	$-f$		f	$-f$								j		
17		y		$-f$				f			f	$-f$							j	
18		z	f		$-f$								f	$-f$						j

$$f = Zd$$
$$g = Yb$$
$$h = \frac{(Y-4)}{(Y+4)}$$
$$i = d$$
$$j = \frac{(4-Z)}{(4+Z)}$$

where Y and Z take a subscript appropriate to the corresponding stub. For example,

$$S_{29} = c = \frac{-Y_x}{2(4+Y_x)} - \frac{Z_y}{2(4+Z_y)}$$

since ports 2 and 9 are both associated with E_x and H_y.

Note that for $Y = Z = 0$, the scattering properties of (16) become the same as (14), as would be expected.

IV. Output and Excitation

The pulses contributing to the E_x field are at ports 1, 2, 9, 12, and 13. From Table I, the capacitance of the transmission-line legs associated with ports 1, 2, 9, and 12 is $Y_0 \Delta t/2$, and the capacitance of the transmission-line stub associated with port 13 is $Y_x Y_0 \Delta t/2$.

The total charge injected by voltage pulses incident on the ports is therefore given by

$$Q = \frac{Y_0 \Delta t}{2}\left(V_1^i + V_2^i + V_9^i + V_{12}^i + Y_x V_{13}^i\right) \tag{17}$$

where V_n^i is the incident voltage pulse on port n.

Conservation of current (or charge) means that the total charge leaving the ports is also given by (17) and can be checked by evaluating

$$V_1^r + V_2^r + V_9^r + V_{12}^r + Y_x V_{13}^r$$

from (16).

Thus, during a whole timestep, the total charge on the transmission-line legs is

$$Y_0 \Delta t\left(V_1^i + V_2^i + V_9^i + V_{12}^i + Y_x V_{13}^i\right).$$

The total capacitance modeled by the transmission lines is

$$\frac{Y_0 \Delta t}{2}(4+Y_x).$$

Thus, the total voltage V_x in the x direction at the node is given by

$$V_x = 2\left(V_1^i + V_2^i + V_9^i + V_{12}^i + Y_x V_{13}^i\right)/(4+Y_x). \tag{18}$$

The E field is therefore

$$E_x = 2\left(V_1^i + V_2^i + V_9^i + V_{12}^i + Y_x V_{13}^i\right)/u(4+Y_x).$$

A similar analysis may be performed for the other output quantities and the results are

$$E_y = 2\left(V_3^i + V_4^i + V_8^i + V_{11}^i + Y_y V_{14}^i\right)/v(4+Y_y)$$
$$E_z = 2\left(V_5^i + V_6^i + V_7^i + V_{10}^i + Y_z V_{15}^i\right)/w(4+Y_z)$$
$$H_x = 2\left(V_4^i - V_5^i + V_7^i - V_8^i - V_{16}^i\right)/Z_0 u(4+Z_x)$$
$$H_y = 2\left(-V_2^i + V_6^i + V_9^i - V_{10}^i - V_{17}^i\right)/Z_0 v(4+Z_y)$$
$$H_z = 2\left(-V_3^i + V_1^i + V_{11}^i - V_{12}^i - V_{18}^i\right)/Z_0 w(4+Z_z). \tag{19}$$

The total voltages and currents at a node may be excited by examining combinations of incident pulses which excite each separate quantity only. Thus, for example, (16) shows that if unit pulses are incident on ports 1, 2, 9, 12, and 13, then unit impulses are reflected into these ports and there are no reflections into any other ports. Thus, the nodal voltage V_x and hence E_x are excited, and from (18) the value of V_x is 2. It can be deduced, therefore, that if the separate field components of $\boldsymbol{E}$ and $\boldsymbol{H}$ are to be excited, one possible set of incident pulses is given by

$$V_1^i = (uE_x + wZ_0 H_z)/2$$
$$V_2^i = (uE_x - vZ_0 H_y)/2$$
$$V_3^i = (vE_y - wZ_0 H_z)/2$$
$$V_4^i = (vE_y + uZ_0 H_x)/2$$
$$V_5^i = (wE_z - uZ_0 H_x)/2$$
$$V_6^i = (wE_z + vZ_0 H_y)/2$$
$$V_7^i = (wE_z + uZ_0 H_x)/2$$
$$V_8^i = (vE_y - uZ_0 H_x)/2$$
$$V_9^i = (uE_x + vZ_0 H_y)/2$$
$$V_{10}^i = (wE_z - vZ_0 H_y)/2$$
$$V_{11}^i = (vE_y + wZ_0 H_z)/2$$
$$V_{12}^i = (uE_x - wZ_0 H_z)/2$$
$$V_{13}^i = uE_x/2$$
$$V_{14}^i = vE_y/2$$
$$V_{15}^i = wE_z/2$$
$$V_{16}^i = -Z_x Z_0 u H_x/2$$
$$V_{17}^i = -Z_y Z_0 v H_y/2$$
$$V_{18}^i = -Z_z Z_0 w H_z/2.$$

For example, if only the field $E_x = 1$ is excited, then the following incident pulses are required:

$$V_1^i = u/2 \quad V_2^i = u/2 \quad V_9^i = u/2 \quad V_{12}^i = u/2 \quad V_{13}^i = u/2.$$

V. Propagation Properties

A full propagation analysis of the symmetrical condensed node requires the determinant of the scattering matrix to be expressed in symbolic form, and this has not yet been done. However, it is possible to make some simple observations for plane-wave propagation in two directions for the node without stubs.

Consider a y-polarized plane wave traveling in the positive x direction with unit pulses incident on port 3 of nodes in a given $y-z$ plane, i.e.,

$$V_3^i = 1$$
$$V_n^i = 0 \qquad n \neq 3.$$

From (14), the reflected pulses are

$$V_1^r = V_4^r = V_8^r = -V_{12}^r = \tfrac{1}{2}$$
$$V_n^r = 0 \qquad \text{for all other } n.$$

Thus, there is no energy reflected into the backward direction (port 3) or transmitted into the forward direction (port 11).

However, similar excitations on neighboring nodes clearly give the following incident pulses at the next timestep:

$$V_4^i = V_8^i = -V_1^i = V_{12}^i = \tfrac{1}{2}$$
$$V_n^i = 0 \qquad \text{for all other } n.$$

Equation (14) now gives the reflected pulses as

$$V_{11}^r = 1$$
$$V_n^r = 0 \qquad n \neq 11.$$

Thus, all of the energy entering a cube of space at port 3 exits the cube at port 11 after two timesteps. This means that the velocity of waves on the transmission-line structure is half the velocity of pulses on the individual transmission lines. This is to be expected since C_x in (3) and L_z in (7) are given by

$$C_x = 2C_d \Delta l$$
$$L_z = 2L_d \Delta l$$

where C_d and L_d are the capacitance and inductance per unit length of the four link transmission lines of a cube $u = v = w = \Delta l$. The velocity of low-frequency bulk waves on the expanded-node mesh is also half of the pulse velocity. The remarkable fact for the symmetrical condensed node with no stubs is that the velocity is constant for all frequencies and there is no cutoff of the waves in this direction. This should be compared with the cutoff value of $\Delta l/\lambda = 1/3$ for along-axis propagation for the expanded-node mesh [15].

It is also possible to study a y-polarized plane wave traveling at 45° to the x and z axes by considering pulses entering ports 3 and 4 simultaneously. Thus,

$$V_3^i = V_4^i = 1$$
$$V_n^i = 0 \qquad \text{for all other } n.$$

This time, (14) gives

$$V_1^r = V_3^r = V_4^r = V_5^r = -V_7^r = V_8^r = V_{11}^r = -V_{12}^r = \frac{1}{2}.$$

The mesh is now behaving like two independent two-dimensional series node meshes. Propagation analysis for this structure shows that the velocity of bulk waves at low frequencies on this structure is $1/\sqrt{2}$ times that of free space [15]. Bearing in mind that the distance in three dimensions is $1/\sqrt{2}$ times greater at 45°, the low-frequency effective velocity on the three-dimensional structure is again $1/2$. The cutoff frequency for the structure is $\Delta l/\lambda = 1/2$, which is the same as for the expanded-node mesh for propagation in this direction [15].

Thus, for these two directions of propagation, it can be concluded that at 45° the dispersion in the symmetrical condensed-node mesh is the same as that in the expanded-node mesh, whereas at 0°, where dispersion is at its worst in the expanded-node mesh, there is no dispersion at all in the symmetrical-condensed-node mesh.

VI. Concluding Remarks

The symmetrical condensed node has been in use for some time now and has received extensive and exhaustive tests. The results in [16] confirm that the new node is more accurate than both the expanded-node mesh and the symmetrical-node mesh. The new mesh is easier to use and has already been connected to three-dimensional graphics modeling packages for automatic data preparation. It has also proved to be much easier to use in conjunction with diakoptics using space and time approximations [17].

The relationship between the expanded-node mesh and the finite-difference method has been examined in some detail [18], and under certain circumstances it is possible for the two methods to be equivalent. Any equivalence between the symmetrical-condensed-node mesh and a finite-difference routine is not immediately obvious, however, and must therefore be the subject of further study.

Acknowledgment

Symmetrical condensed nodes were a topic of much discussion between the author and Prof. R. L. Beurle of the Department of Electrical and Electronic Engineering, University of Nottingham, in 1974 and 1975. This contribution and notes written by Prof. Beurle at that time are gratefully acknowledged.

References

[1] P. B. Johns, "The art of modeling," *IEE Trans. Electron. Power*, vol. 25, no. 8, pp. 565–569, Aug. 1979.

[2] W. J. R. Hoefer, "The transmission-line matrix method—Theory and applications," *IEEE Trans. Microwave Theory Tech.*, vol. MTT-33, pp. 882–893, Oct. 1985.

[3] S. Akhtarzad and P. B. Johns, "The solution of Maxwell's equations in three space dimensions and time by the TLM method of numerical analysis," *Proc. Inst. Elec. Eng.*, vol. 122, no. 12, pp. 1344–1348, Dec. 1975.

[4] P. B. Johns and G. Butler, "The consistency and accuracy of the TLM method for diffusion and its relationship to existing methods," *Int. J. Num. Methods Eng.*, vol. 19, pp. 1549–1554, 1983.

[5] K. S. Yee, "Numerical solution of initial boundary value problems involving Maxwell's equations in isotropic media," *IEEE Trans. Antennas Propagat.*, vol. AP-14, no. 3, pp. 302–307, May 1966.

[6] A. Taflove and M. E. Brodwin, "Numerical solution of steady-state electromagnetic scattering problems using the time-dependent Maxwell's equations," *IEEE Trans. Microwave Theory Tech.*, vol. MTT-23, pp. 623–630, Aug. 1975.

[7] P. B. Johns, and K. Akhtarzad, "The use of time domain diakoptics in time discrete models of fields," *Int. J. Num. Methods Eng.*, vol. 17, pp. 1–14, 1981.

[8] P. B. Johns and K. Akhtarzad, "Time domain approximations in the solution of fields by time domain diakoptics," *Int. J. Num. Methods Eng.*, vol. 18, pp. 1361–1373, 1982.

[9] P. B. Johns, and Y. Rahhal, "The use of diakoptics for the numerical simulation of the penetration of time domain fields in

aircraft," in *Int. Conf. Electromagnetic Compatibility* (University of Surrey), IERE Publication No. 56, Sept. 21–23, 1982.

[10] P. Saguet and E. Pic, "Utilisation d'un nouveau type de noeud dans la method TLM en 3 dimensions," *Electron. Lett.*, vol. 18, no. 11, pp. 478–480, May 1982.

[11] P. Saguet, and S. Tedjini, "Method des lignes de transmission en trois dimensions: modification du processus de simulation," *Ann. Telecommun.*, vol. 40, nos. 3–4, pp. 1–8, Mar.–Apr. 1985.

[12] A. Amer, "The condensed node TLM method and its application to transmission in power system," Ph.D. thesis, Nottingham University, 1980.

[13] P. B. Johns, "Ideal transformers and guage transformations in lumped network models of electromagnetic fields," *Proc. Inst. Elec. Eng.*, vol. 129, pt. A, no. 6, Aug. 1982.

[14] R. E. Collin, *Foundations for Microwave Engineering.* New York: McGraw Hill, 1966.

[15] C. R. Brewitt-Taylor and P. B. Johns, "On the construction and numerical solution of transmission-line and lumped network models of Maxwell's equations," *Int. J. Num. Methods Eng.*, vol. 15, pp. 13–30, 1980.

[16] R. Allen, A. Mallik, and P. B. Johns, "Numerical results for the symmetrical condensed TLM node," pp. 378–382, this issue.

[17] P. B. Johns and A. Mallik, "EMP response of aircraft structures using TLM," presented at 6th Symp. Tech. Exhibition Electromagnetic Compatibility, Zurich, March 5–7, 1985.

[18] P. B. Johns, "On the relationship between TLM and finite-difference methods for Maxwell's equations," *IEEE Trans. Microwave Theory Tech.*, vol. MTT-35, pp. 60–61, Jan. 1987.

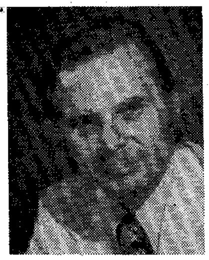

Peter B. Johns was born in Newport, Wales, in 1938. He received the B.Sc. (eng.) degree in electrical engineering and the M.Sc. degree in physics from London University, England, in 1964 and 1966, respectively, and the Ph.D. degree from Nottingham University, England, in 1973.

From 1964 to 1967, he was with British Telecom Research Laboratories at Dollis Hill, London, where he worked on interference problems associated with satellite communication systems. In 1967, he was appointed Lecturer in the Department of Electrical and Electronic Engineering, University of Nottingham, and he is now Professor of Information Systems and Head of Department. He was a visiting Research Associate at the University of Manitoba in 1975/76.

Dr. Johns has originated and developed the modeling procedure TLM for computer simulation of electromagnetic waves, diffusion processes, and network analysis. He has published many papers on the subject, and in 1976 he won the Electronics Division Premium of the Institution of Electrical Engineers. He is Managing Director of a small company set up in Nottingham to provide a numerical modeling service for industry. The electromagnetic applications of TLM presently include the areas of EMP/EMC and microwave tube design.